

“Direct”, “inverted” and “superdirect” sigma bonds: substituent angles and bond energy. The case of the CC bonds in hydrocarbons.

Rubén Laplaza,^[b] Julia Contreras-García^[c], Franck Fuster^[c], François Volatron^[c], and Patrick Chaquin*^[a]

Abstract. The A-A dissociation energy with respect to geometry frozen fragments (BE) of has been calculated for AH_n-AH_n models (C_2H_6 , Si_2H_6 , Ge_2H_6 and N_2H_4) as a function of $\theta = H-A-A$ angles. Following a sigmoidal variation, BE decreases rapidly when θ decreases to yield “inverted bonds” for $\theta < 90^\circ$ and finally nearly vanishes. On the contrary BE increases when θ increases with respect to the equilibrium value; we propose the term of “superdirect” to qualify such bonds. This behaviour has been qualitatively interpreted in the case of C_2H_6 by the variation of the overlap of both s+p hybrids. The BE of one C-H bond in CH_3 behaves similarly as function of its H-C-H angle with the other three hydrogen atoms. The concept of inverted/direct/superdirect bond is generalized to any CC sigma bond in hydrocarbons and can be characterized by the mean angle value $\langle\theta\rangle$ of this bond with substituents (multiple-bonded substituents are considered as several substituents). This applies as well to formal single bonds as to sigma bonds in a formally multiple bond.

Using dynamic orbital forces (DOF) as indices, the intrinsic bond energies are studied as a function of $\langle\theta\rangle$ for a panel of 33 molecules. In formally single bonds, this energy decreases from the “superdirect” bonds in butadiyne, tetrahydrotetrahedrane and related compounds ($\langle\theta\rangle > 125^\circ$), to the “inverted bonds” ($\langle\theta\rangle < 90^\circ$) in bicyclobutane and [1.1.1]propellane for which it is nearly vanishing. The ring strain in cyclopropane and cyclobutane can be interpreted in terms of directness/superdirectness of C-C and C-H bonds. Sigma bonds in formally multiple bonds are found inverted or near inverted and thus are significantly weaker than standard single bonds.

^[a] Pr. P. Chaquin

Laboratoire de Chimie Théorique (LCT)
Sorbonne Université, CNRS, F-75005 Paris
E-mail : chaquin@lct.jussieu.fr

^[b] R. Laplaza

Laboratoire de Chimie Théorique (LCT)
Sorbonne Université, CNRS, F-75005 Paris

Departamento de Química Física
Universidad de Zaragoza
50009 Zaragoza, Spain

[c] Dr. J. Contreras-García, Dr. F. Fuster, Dr. F. Volatron
Laboratoire de Chimie Théorique (LCT)
Sorbonne Université, CNRS, F-75005 Paris

Introduction

In a recent publication, we revisited the properties of the so-called “inverted bond” in [1.1.1]propellane (Figure 1).¹ In previous works, its energy was evaluated to ca. 60 kcal/mol,² and it was identified as a charge-shift bond.³ We concluded on the contrary that the corresponding sigma bond has a negligible energy and that the bonding arises only from π (or “wing”, or “banana”) interactions through the three CH₂ bridges. This publication was followed by a comment by Braïda et al.⁴

Let us recall that inverted bonds result from the overlap of s+p hybrids by their smaller lobe (Figure 1), by contrast to “normal” or “direct” bonds in which the overlap occurs between their bigger lobes. In ref 1, we used C₂H₆ models to mimic *in silico* the CC bond inversion by decreasing the HCC from its optimized value close to 110° down to 70°. The CC dissociation energy, computed with respect to geometry frozen CH₃ moieties, was found to decrease rapidly and by extrapolation should tend to zero for HCC = 60°.

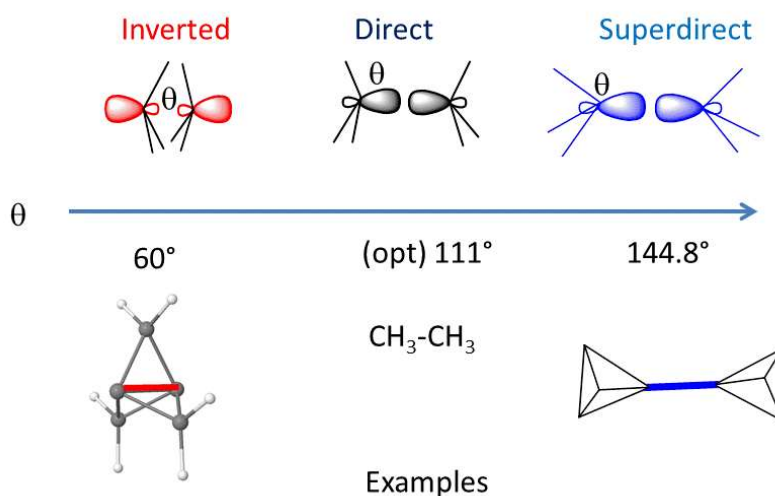


Figure 1. “Inverted”, “direct” and “superdirect” bonds according to the θ angle of substituents. [1.1.1]Propellane, ethane and tetrahedryltetrahydrodane exemplify these three types of bonds respectively.

In the present work, we will, in a first step, allow the HCC angle of C₂H₆ increase significantly above its optimized value to build bonds which are in a sense the contrary of the inverted bonds. We propose the term of “superdirect” for such bonds. Thus, as displayed in Figure 1, the bonds can be classified into “inverted”, “direct” and “superdirect”. Then the influence of

substituent angles on bond energy in Si₂H₆, Ge₂H₆, N₂H₄ and H₃C-H models will be studied from the same point of view.

In a second step, we will generalize the notion of invertedness/directness/superdirectness to any σ CC bond in hydrocarbons by setting a “mean substituent angle” $\langle\theta\rangle$. We will consider the relation of this parameter with bond strength in a panel of 33 molecules. For this purpose, the Dynamic Orbital Forces (DOF) will be used as indices of intrinsic bond energy and as a tool of σ/π partition.

Computational Details

Geometry optimization and bonding energies with respect to geometry frozen fragments have been calculated at the CCSD(T)/cc-pVQZ level for C₂H₆ and CH₃-H models, and at the MP2/cc-pVTZ level for Si₂H₆, Ge₂H₆ and N₂H₄ ones. The geometry of molecules **1-33** was also optimized at the MP2/cc-pVTZ level. The derivatives of the canonical molecular orbitals were performed, with the same basis set as geometry optimization, by a finite difference of bond lengths of 0.002 Å to 0.004 Å according to the case, thanks to a home-made script. The Gaussian09 program was used throughout this work.⁵

Results and discussion

1. C₂H₆ models

1.1. Influence of HCC angles on CC bond energy in C₂H₆

The following models were first considered (Figure 2). In model 1, all six $\theta = \text{HCH}$ angles are varied from 70° to 145°; in model 2 three angles θ' are kept equal to their optimized value in ethane (111.2°) and three other θ angles are varied from 60° to 140°. After geometry optimization, The C-C bond energy (BE) with respect to geometry frozen CH₃ moieties has been computed at the CCSD(T)/cc-pVQZ level. (The results for $\theta \leq 111.2^\circ$ are taken from ref. 1).

Table 1. C₂H₆ models 1 and 2. Geometrical parameters R(Å) and bonding energy BE (kcal/mol, with respect to two CH₃ at frozen geometry) as function of θ ; R(CH1) refers to CH₃ group with variable $\theta =$ HCC angle; R(CH2) refers to CH₃ group of constant $\theta' =$ HCC angle; CCSD(T)/cc-pvQZ level of calculation.

C ₂ H ₆ model 1								
θ	140°	130°	120°	opt (111.2°)	100°	90°	80°	70°
R(CC)	1.422	1.448	1.483	1.527	1.628	1.830	2.231	2.9
R(CH)	1.135	1.111	1.097	1.091	1.085	1.079	1.079	1.089
BE	152.8	145.0	131.6	114.1	81.6	44.5	15.4	5.6
C ₂ H ₆ model2								
θ	140°	130°	120°	opt (111.2°)	100°	90°	80°	70°
R(CC)	1.485	1.492	1.508	1.527	1.5760	1.648	1.766	1.937
R(CH1)	1.138	1.112	1.098	1.091	1.085	1.082	1.082	1.091
R(CH2)	1.089	1.089	1.090	1.091	1.091	1.091	1.090	1.088
BE	133.6	128.9	121.5	114.1	96.2	75.6	52.2	33.8

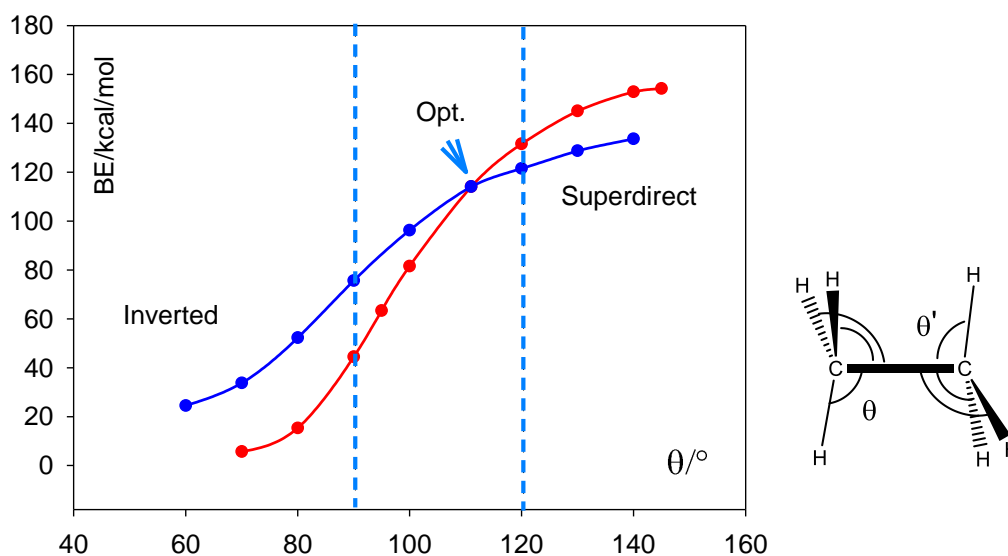


Figure 2. CC bonding energy (BE) in C₂H₆; model 1 (red curve) $\theta = \theta'$; model 2 (blue curve) $\theta' = 111.2^\circ$ (optimized value in ethane).

In both models 1 and 2, BE decreases rapidly when θ decreases from the optimized geometry to yield an inverted bond; it increases slowly when θ increases to yield a superdirect bond from the (arbitrary) limit of 120° . As expected, the effects are less marked for model 2 in which only one CH₃ is deformed. In three additional calculations (model 3), θ and θ' have a constant sum (220°), with $\theta = 100^\circ, 90^\circ, 80^\circ$ and thus $\theta' = 120^\circ, 130^\circ, 140^\circ$ respectively; this way, one CH₃ tends towards “invertedness” whereas the other one tends to “superdirectness”. The following BE are found: 107 kcal/mol for $\theta = 100^\circ$ and $\theta' = 120^\circ$; 93 kcal/mol for $\theta = 90^\circ$ and $\theta' = 130^\circ$; 77 kcal/mol for $\theta = 80^\circ$ and $\theta' = 140^\circ$. As expected

from the preceding results, the loss of BE due to a smaller angle value is only partly compensated by its raise due to the larger value of the other one. Figure 3 reveals a net correlation of the bonding energy as a function of $\langle\theta\rangle$, mean value of HCC angles, in the three C_2H_6 models ($\langle\theta\rangle = \theta$ for model 1; $\langle\theta\rangle = \frac{1}{2}(\theta + \theta')$ for models 2 and 3).

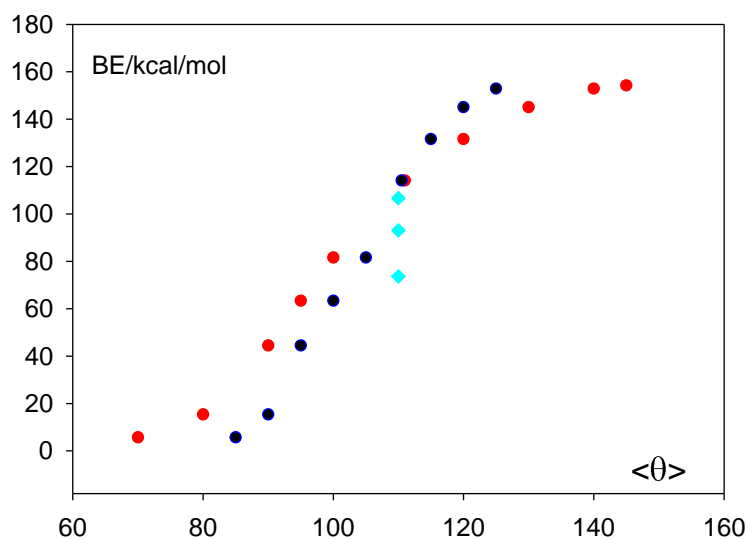


Figure 3. CC bond energy in C_2H_6 as a function of $\langle\theta\rangle$ mean value of H-C-C angle: model 1 (red) model 2 (blue), model 3 (cyan).

1.2 Qualitative interpretation

The overall sigmoidal shape of BE curve as a function of θ can be interpreted qualitatively by an approximate evaluation of the overlap of both s+p hybrids, which we detail in the case of model 1.

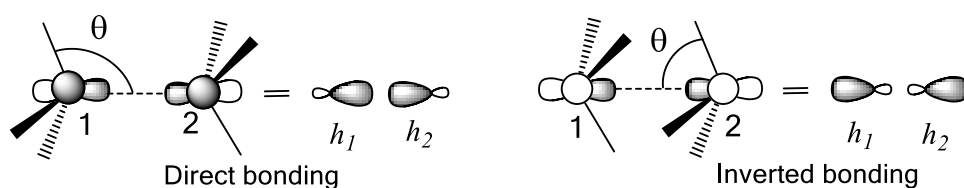


Figure 4. Overlap in direct and inverted bonding

The hybrids h_1 and h_2 are written as:

$$h_1 = \alpha s_1 + \beta p_1$$

$$h_2 = \alpha s_2 + \beta p_2$$

with $\alpha^2 + \beta^2 = 1$. Setting $\beta > 0$:

$$\alpha < 0 \text{ for } \theta < 90^\circ$$

$$\alpha = 0 \text{ for } \theta = 90^\circ$$

$$\alpha > 0 \text{ for } \theta > 90^\circ$$

The theoretical limits of θ are 0° , with $\alpha = -\beta = -1/\sqrt{2}$ and 180° , with $\alpha = \beta = 1/\sqrt{2}$. The corresponding hybridization states can be referred to as sp^{-1} and sp respectively. Between these limits, the following hybridization states are encountered: sp^{-2} ($\alpha = -1/\sqrt{3}$), sp^{-3} ($\alpha = -1/2$), s^0p ($\alpha = 0$), sp^3 ($\alpha = 1/2$), sp^2 ($\alpha = 1/\sqrt{3}$). The following values of α are obtained with the minimal basis STO-3G for CH_3 and various θ (Table 2).

Table 2. Coefficient α of the s AO in the CH_3 hybrid as a function of θ angle (see Figure 4)

θ	60	70	80	90	100	110	120	130
α	-0.601	-0.483	-0.294	0.000	0.294	0.483	0.601	0.643

The overlap S of h_1 and h_2 is:

$$S = \langle \alpha s_1 + \beta p_1 | \alpha s_2 + \beta p_2 \rangle = \alpha^2 \langle s_1 | s_2 \rangle + \beta^2 \langle p_1 | p_2 \rangle + 2\alpha\beta \langle s_1 | p_2 \rangle$$

To a first approximation, the three atomic overlaps are close to $S_0 = 0.3$ at CC distances of 1.4-1.6 Å:

$$S \approx S_0(\alpha^2 + \beta^2 + 2\alpha\beta) = S_0(1 + 2\alpha\beta)$$

The overlap S as a function of θ has the same sigmoidal shape as the bonding energy (Figure 5(a)). Moreover, though the crudeness of the approximations involved, the bonding energy is nearly linearly connected to S , except for the highest θ values (Figure 5 (b)).

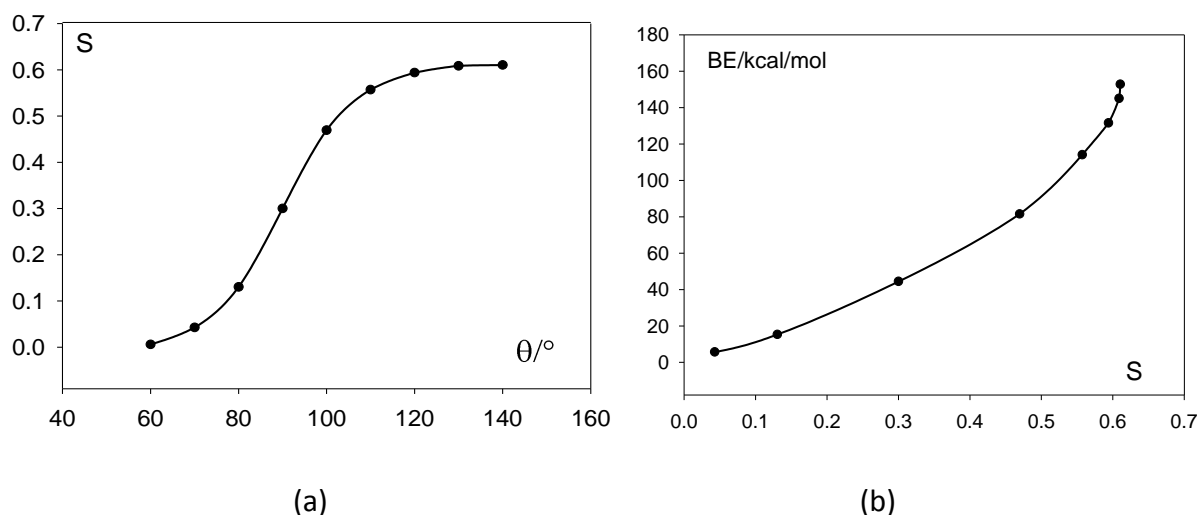


Figure 5. (a) Variation of overlap S with θ in C_2H_6 model 1, for a CC distance $\approx 1.5 \text{ \AA}$. (b) Variation of CC bonding energy BE (from Table 1) as a function of S .

It appears that the bonding energy is closely related to the overlap at the standard bond length distance ($\approx 1.5 \text{ \AA}$), controlled itself by the hybridization state of the CH_3 semi-occupied AO according to the θ angle of deformation. Indeed, the final optimized CC distance involves other parameters as evidenced by energy decomposition analysis.⁶

2. Other models: Si_2H_6 , Ge_2H_6 , N_2H_4 and CH_4

Though we are mainly interested in CC bonds in this work, we examined several models involving other bonds to compare their behaviour when angle constraints are imposed.

Two systems Si_2H_6 and Ge_2H_6 have been studied in the same way as C_2H_6 model 1 at the MP2/cc-pVTZ level. The geometrical properties and the bonding energies of Si-Si and Ge-Ge bonds respectively are reported in Table 3. Figures 6(a) and 6(b) display the variation of BE as a function of the θ angle.

Table 3. Si_2H_6 and Ge_2H_6 model. Geometrical parameters R (Å) and bonding energy BE (kcal/mol with respect to two AH_3 in frozen geometry) as functions of θ ; opt = 110.4° (Si_2H_6); opt= 110.4° (Ge_2H_6); MP2/cc-pVTZ level of calculation.

Si_2H_6 model 1									
θ	140°	130°	120°	opt	100°	90°	80°	70°	60°
R(SiSi)	2.242	2.289	2.321	2.351	2.394	2.492	2.726	3.038	3.287
R(SiH)	1.517	1.497	1.486	1.481	1.477	1.471	1.469	1.483	1.501
BE	83.9	81.8	80.2	76.8	68.8	45.6	15.3	1.1	-0.4
Ge_2H_6 model 1									
θ	140°	130°	120°	opt	100°	90°	80°	70°	60°
R(GeGe)	2.271	2.316	2.357	2.398	2.458	2.568	2.800	3.068	3.281
R(GeH)	1.554	1.536	1.525	1.518	1.513	1.505	1.505	1.523	1.546
BE	83.8	81.3	79.0	74.5	65.1	44.1	17.7	6.0	5.7

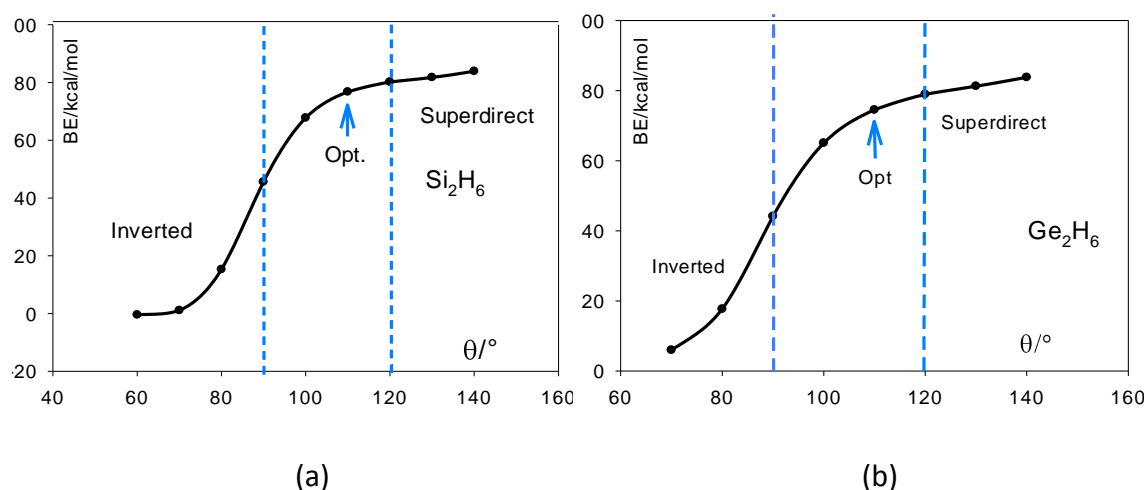


Figure 6. Central bond energies of Si_2H_6 (a) and Ge_2H_6 (b) as functions of θ angles (H-Si-Si and H-Ge-Ge respectively).

The two curves are very similar. They have also the same general shape as for C_2H_6 , but with a weaker BE increase in the superdirect region ($\theta > 120^\circ$). It appears that the decrease of the ns-np gap in these both species, with respect to C_2H_6 , is only of minor consequence as compared to the angle variation.

The BE of the NN bond of $\text{NH}_2\text{-NH}_2$ in D_{2d} symmetry was also studied as a function of $\theta = \text{HNN}$ angles. The dissociation energy was computed with respect to geometry frozen NH_2 fragments in their 2A_1 state. As a matter of fact, N-N bond breaking results in the formation of two NH_2 radicals possessing a lone pair in a pure 2p AO and a semi occupied s+p hybrid. In its optimized geometry, this state lies ca. 34 kcal/mol above the 2B_1 ground state.⁷ Thus the

value of BE in geometry optimized N_2H_4 lies at 68 kcal above the NN dissociation energy into $2NH_2$ in their ground state.

Table 4. N_2H_4 in D_{2d} symmetry. Geometrical parameters R (Å) and bonding energy BE (kcal/mol with respect to two NH_2 in frozen geometry) as functions of θ ; opt = 119.9° ; MP2/cc-pVTZ level of calculation.

θ	$N_{2H_4} D_{2d}$									
	150°	130°	opt	110°	100°	90°	80°	70°	60°	
R(NN)	1.299	1.326	1.363	1.420	1.507	1.647	1.852	2.054	2.196	
R(NH)	1.039	1.008	1.000	0.995	0.993	0.992	0.997	1.008	1.024	
BE	166.7	156.63	141.0	119.0	91.0	58.6	31.0	16.3	11.2	

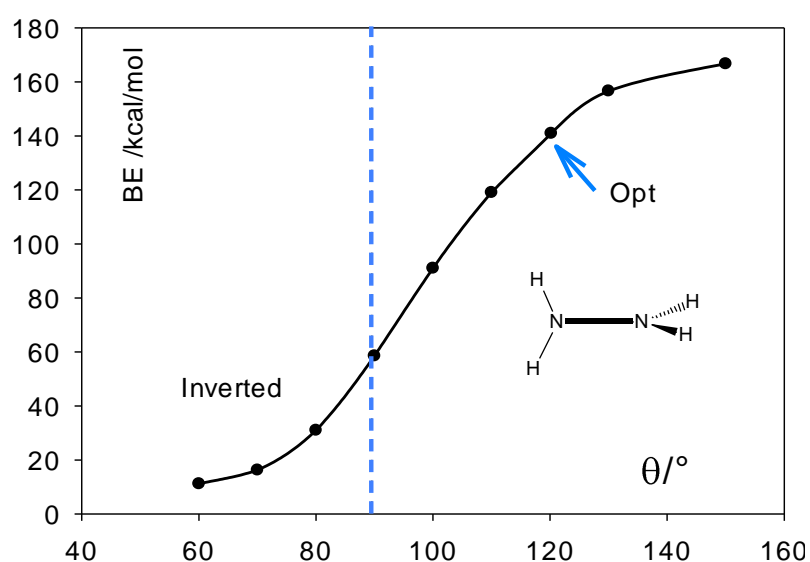


Figure 7. NN bond energy in N_2H_4 (D_{2d}) as a function of $\theta = H-N-N$ angles.

Finally, we studied the influence in CH_4 of three $\theta = HCH$ angles on the energy of the fourth C-H bond. Results in Table 5 and Figure 8 are similar to preceding ones, especially to model 2, because only three valence angles are involved in this model.

Table 5. H₃C-H. Geometrical parameters R (Å) and bonding energy BE of CH (kcal/mol, with respect to H and CH₃ at frozen geometry) as function of θ ; opt = 109.5°; CH1 refers to H in CH₃ group ; CCSD(T)/cc-pVQZ level of calculation.

		H ₃ C-H								
θ	140°	130°	120°	opt	100°	90°	80°	70°	60°	
R(CH)	1.063	1.068	1.076	1.087	1.105	1.132	1.174	1.229	1.290	
R(CH1)	1.134	1.108	1.095	1.087	1.085	1.084	0.876	1.003	1.130	
BE	138.4	134.1	127.7	119.4	107.5	90.6	70.8	54.1	44.9	

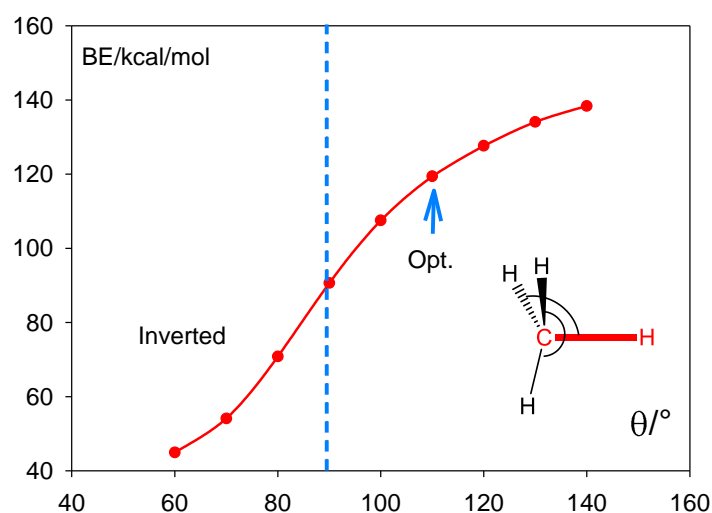


Figure 8. CH bonding energy in H₃C-H (red bond) as a function of θ = HCH angles.

Such models confirm the conclusions of the C₂H₆ studies. All studied models agree with the fact that the bond energy is strongly dependent on the substituent angles: it decreases rapidly with the inverted character of the bond and increases more slowly with the superdirect character of the bond. These phenomena are related to the variation of the hybridization of the s+p AOs overlapping in the bond formation, controlled by these angles. Specifically, BE increases with the s (algebraic) coefficient in the s+p hybrids. This result is well-known for direct C-H bonds with aliphatic (sp³), ethylenic (sp²) and acetylenic (sp) carbons. It has been also pointed out with direct C-C bonds⁸, for example regarding the strong central bond of tetrahedryltetraedrane.⁹

3. Inverted, direct, and superdirect bonds: generalization for sigma CC bonds in hydrocarbons

3.1. Mean angle $\langle\theta\rangle$ of substitution

The preceding models preserve a symmetry axis along the bond under scrutiny with equal angles of H substituents on each heavy atom. We will now extend the inverted/direct/superdirect character to any σ CC bond in hydrocarbons, as well for formally single bonds as for σ bonds in formally multiple bonds. For this purpose, we define $\langle\theta\rangle$ as mean value of the angles of the six substituents on both carbon atoms; the π bonds will be treated as σ ones in this calculations. Two examples are given in Figure 9.

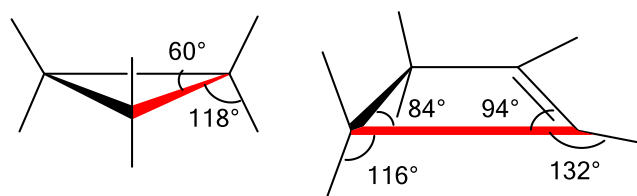


Figure 9. Calculation of $\langle\theta\rangle$ angle of the red bond of cyclobutane and cyclobutene.

In cyclopropane, the red bond has 4 H at 118° and two C at 60° , yielding $\langle\theta\rangle \approx 99^\circ$. In cyclobutene, the red bond is considered as having 2 C at 94° , 1 H at 132° , 1 C at 84° and 2H at 116° yielding $\langle\theta\rangle = 106^\circ$. This way, the central C-C bond in butadiyne $\text{H}-\text{C}\equiv\text{C}-\text{C}\equiv\text{C}-\text{H}$ has the $\langle\theta\rangle$ theoretical maximum value of 180° . In formally multiple bonds, the $\langle\theta\rangle$ angle is determined in a similar way. For example, in acetylene $\text{H}-\text{C}\equiv\text{C}-\text{H}$, the σ CC bond is considered as having 4 C at 0° and 2 H at 180° , yielding $\langle\theta\rangle = 60^\circ$.

3.2. Dynamic orbital forces as indices of intrinsic bond energy

In most of cases, the BE of C-C bond cannot be longer computed in the same way as in the first section. Thus we will use the dynamic orbital forces (DOF)¹⁰ as indices of bond energies. The derivative of the i^{th} canonical MO energy ε_i with respect to a bond length ($R(\text{CC})$ in the case of a CC bond) has already been used to characterize the bonding/antibonding character of the MO with respect to this bond.¹¹ The sum Σ_{tot} of these derivatives over occupied MOs by n_i electrons can be decomposed into σ (Σ_σ) and π (Σ_π) components:

$$\Sigma_{tot} = \sum_i^{occ} n_i \frac{d\varepsilon_i}{dR(CC)} = \sum_j^{\sigma occ} n_j \frac{d\varepsilon_j}{dR(CC)} + \sum_k^{\pi occ} n_k \frac{d\varepsilon_k}{dR(CC)} = \Sigma_{\sigma} + \Sigma_{\pi}$$

It has been recognized that Σ_{tot} is an index of the “bond strength”, as far as the molecule is satisfactorily described at the Hartree-Fock level.^{12,13} However, it is an intrinsic quantity of the system whereas the bond energy dissociation with respect to geometry frozen fragments (BE) considered in the preceding sections involves the electronic relaxation of fragments and thus some reorganization energy. This tends to lower BE with respect to the intrinsic bond energy. But this difference should be small in symmetrical or near symmetrical systems, which need only a negligible electron transfer in the bond formation. Indeed, a good correlation between Σ_{tot} and BE is found for CC bonds. In Figure 10, we report Σ_{tot} for C_2H_6 (model 1) and various CC bonds (taken from ref 10). We observe an excellent linear correlation of BE of CC bonds and Σ_{tot} in the series C_2H_2 , C_2H_4 , C_6H_6 , C_2H_6 and C_3H_6 . In C_2H_6 (model 1), the variation of Σ_{tot} according θ is no longer linear, but nevertheless regular and monotonic. We thus assume that Σ_{tot} is a reliable index to classify the CC intrinsic bond energies in hydrocarbons, and that Σ_{σ} and Σ_{π} reflect the relative σ and π components of this energy.

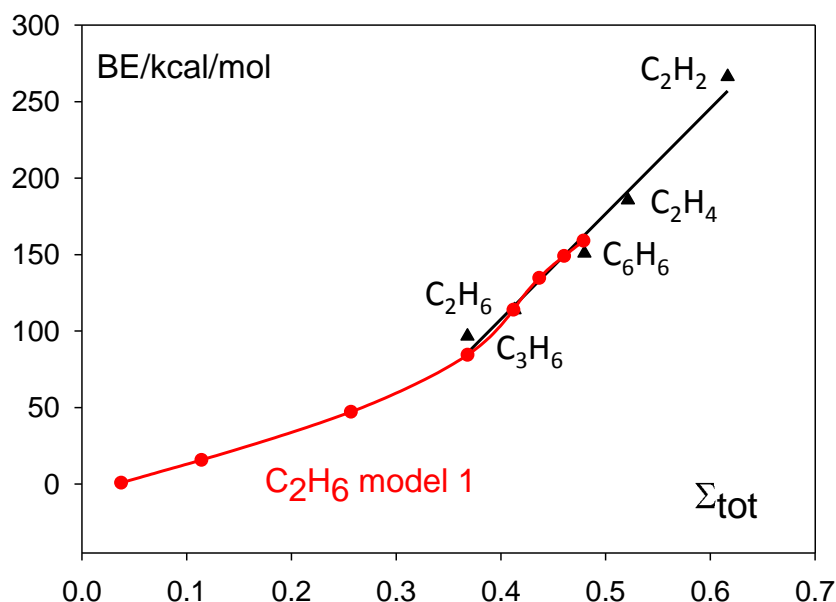


Figure 10. Bonding energy with respect to geometry frozen fragments (MP2/cc-pVTZ) as a function of Σ_{tot} (a.u.).

A correlation between BE and Σ_{tot} is also obtained for Si-Si, Ge-Ge and N-N bonds in the Si_2H_6 , Ge_2H_6 and N_2H_4 models (Figure 11) for which the bonding energy as a function of θ has been studied in section 3.

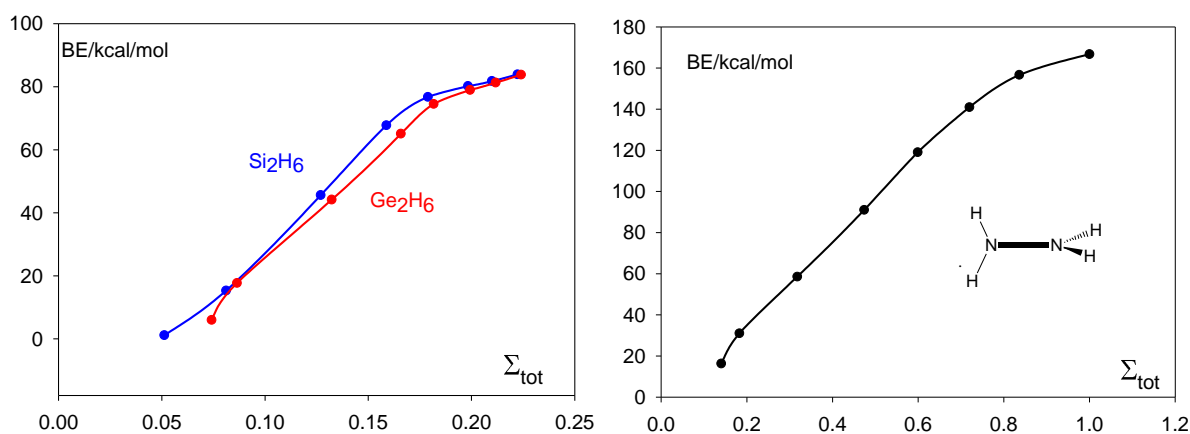


Figure 11. Correlation between BE, for various θ , and Σ_{tot} (a.u.) for Si_2H_6 , Ge_2H_6 and N_2H_4 (see section 2).

3.3. Sigma CC bond energy and mean angle of substituents

In Table 6, we report the values of Σ_{tot} , Σ_{σ} and Σ_{π} in a panel of formally single C-C bonds by order of decreasing values of $\langle\theta\rangle$ from 180° to 60° . The concepts of directness/invertedness concerns σ bonds, and thus we will be interested mainly in the Σ_{σ} component, though Σ_{tot} and Σ_{π} could also offer useful information.

Table 6. Values of Σ_{tot} , Σ_{σ} , Σ_{π} (a.u.); % of Σ_{π} in Σ_{tot} and the corresponding values of $\langle\theta\rangle$ (°) for formally single C-C bonds (TET = tetrahedral; BCP = bicyclopentyl; CUB = cubyl).

Label	Molecule	Σ_{tot}	Σ_{σ}	Σ_{π}	% π	$\langle\theta\rangle$
1	HC≡C—C≡CH	0.513	0.450	0.064	12.4	180
2	TET—C≡CH	0.527	0.437	0.090	17.1	163
3	TET—TET	0.468	0.447	0.021	4.5	145
4	CH ₃ —C≡CH	0.458	0.415	0.042	9.1	145
5	TET—CH ₃	0.495	0.442	0.053	10.1	128
6	BCP—BCP	0.489	0.434	0.055	11.3	127
7	CUB—CUB	0.478	0.420	0.058	12.1	125
8	CH ₂ =CH—CH=CH ₂	0.478	0.433	0.045	9.4	121
9	CH ₃ —CH=CH ₂	0.418	0.399	0.019	4.5	116
10	Ph—CH ₃	0.415	0.397	0.019	4.6	115
11	tbu—tbu	0.439	0.392	0.048	10.8	111
12	CH ₃ —CH ₃	0.413	0.392	0.021	4.9	111
13	cyclohexane	0.445	0.425 ^a	0.02 ^a	4.5 ^a	110
14	cyclopentane	0.420	0.403	0.017 ^b	4.3	108
15	cyclobutene (2-3)	0.445	0.400	0.045	10.1	106
16	cyclobutene (3-4)	0.404	0.396	0.008	2.0	105
17	cyclobutane	0.408	0.401	0.007 ^b	1.7	103
18	cyclopropane	0.368	0.372	-0.004	-1.1	99
19	cyclopropene	0.281	0.283	-0.002	-2.0	88
20	tetrahydrene	0.353	0.278	0.075	21.2	88
21	bicyclobutane ^c	0.360	0.164	0.196	54.4	82
22	[1.1.1]Propellane ^c	0.275	-0.029	0.304	110.5	60

^a Estimated on the basis of the same Σ_{π} = 0.02 a.u. as **11**. ^b The π MOs have been visually identified, which can lead to some uncertainty ; ^c central bond (see Fig 14).

We observe (Figure 12) a general decrease of Σ_{σ} with $\langle\theta\rangle$, which preserves roughly the sigmoidal shape observed for the models of sections 1 and 3. As a landmark, we report on the same figure the variation of Σ_{σ} for C₂H₆ model 1 (red curve), at the same calculation level.

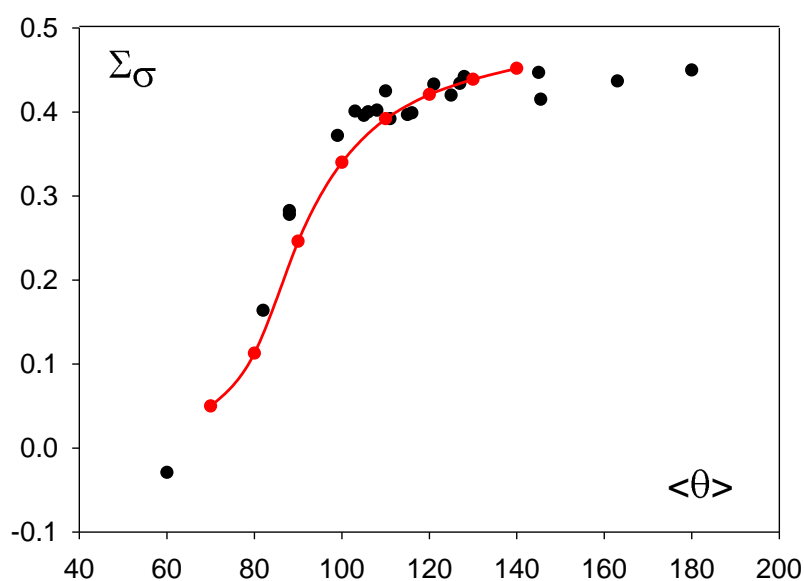


Figure 12. Σ_σ (a.u.) values of molecules 1-20 with respect to the mean substituent angle $\langle\theta\rangle$ ($^\circ$). The red curve corresponds to C_2H_6 model 1.

If ethane **12** is taken as the prototype of “normal” direct CC bond with $\Sigma_\sigma = 0.392$, we note that this value increases up to 0.450 for butadiyne **1** which corresponds to the theoretical maximum value of 180° for $\langle\theta\rangle$.

Bond energies and bond lengths have been calculated for the five superdirect C-C bonds in **1-5** and are reported in Figure 13 together with results of Table 6. Some discrepancies appear in the results of Figure 13. For example, **5** and **2** have a smaller BE than expected from Σ_{tot} . It could be due to their dissymmetry which involves some reorganization energy of the separate fragments (see section 3.2). Nevertheless, molecules **1** and **2** have the strongest bonds and the greater Σ_{tot} values. It can be noted that the high BE of **1** is mainly due to a strong σ bond and not to conjugation, with only 12.4 % π participation to Σ_{tot} . Also, it has been proposed that the short bond of **3** originates equally both from its high s character and from hyperconjugation;¹⁴ but in the present work this term appears weak, with only 4.5 % contribution of π MOs to Σ_{tot} . A value of 12% of π energy has been determined from Energy Decomposition Analysis.¹⁵

The value of Σ_{tot} in tetramethylbutane **11** (0.439 a.u.) suggests that its intrinsic bond energy is greater than that of ethane **12** (0.413 a.u.) though its experimental dissociation energy is significantly smaller (78.6 kcal/mol vs. 90.2 kcal/mol).¹⁶ Nevertheless, the BE of both species

with respect to geometry frozen fragments (MP2/cc-PVTZ) are nearly equal: 113.0 kcal/mol for **11** and 113.9 for **12**. Moreover, the electronic relaxation in Me₃C radicals involves an important stabilization by hyperconjugation, which leads to underestimate the calculated BE with respect to the actual intrinsic value.

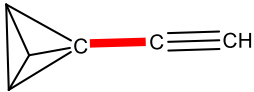
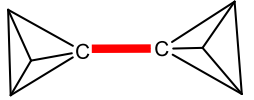
	Σ_{tot}	Σ_s	% π	R(CC)	BE	$\langle\theta\rangle$
 1	0.513	0.450	12.4	1.368	171.8	180
 2	0.527	0.437	17.1	1.394	161.0	163
 3	0.463	0.415	4.5	1.419	150.7	145
 4	0.458	0.415	10.1	1.458	158.0	145
 5	0.495	0.442	10.1	1.476	132.8	128

Figure 13. Some superdirect CC bonds (in red): Σ_{tot} and Σ_s (a.u.); bond energy with respect to geometry frozen fragments (kcal/mol); bond length R(CC) (Å).

In the series of cyclanes, we observe a regular decrease of Σ_{tot} , as the ring strain increases: cyclohexane **13** (0.445), cyclopentane **14** (0.420), cyclobutane **17** (0.408) and cyclopropane **18** (0.368). In the absence of symmetry plane (except for cyclopropane **18**), the π MOs have been identified visually for **14** and **17**. For cyclohexane **13** the σ/π partition becomes problematic because most of the MOs have both types of participation; we assumed that Σ_{π} is close to the value observed for ethane. Under these conditions, a decrease of Σ_{σ} is also observed along the series. The weak π participation in **17** and **18** can be related to their quasi-eclipsed conformation, this participation being nearly zero in eclipsed ethane. Furthermore, it is well known that cyclobutane **17** and cyclopropane **18** have very close strain energies, 26.5 kcal/mol and 27.5 kcal/mol respectively¹⁷, though the three-membered cycle could appear as much more strained. Taken into account that this energy involves all the bonds, it has been suggested that three weaker CC bonds in cyclopropane are

compensated by six stronger CH bonds.^{13a, 18} Indeed, $\langle\theta\rangle(\text{CH}) = 109.5^\circ$ for **17** and 116° for **18**: thus the CH bond in cyclopropane has some superdirect character. Moreover, from Table 5, the energy difference can be evaluated to ca. 5.5 kcal/mol, the same order of magnitude as previous determinations;¹⁹ the corresponding difference for a CC bond with $\langle\theta\rangle$ varying from 103° for **17** to 99° for **18** is about twice (-13.5 kcal/mol from Table 1).

The series of three-membered ring species **18**, **20**, **21** and **22**, compared to ethane **12** (Figure 14) is of a particular interest. The CC bond (in red in Figure 14) undergoes a progressive inversion with $\langle\theta\rangle$ decreasing from 111° (normal bond) to 60° (inverted bond in propellane **22**).

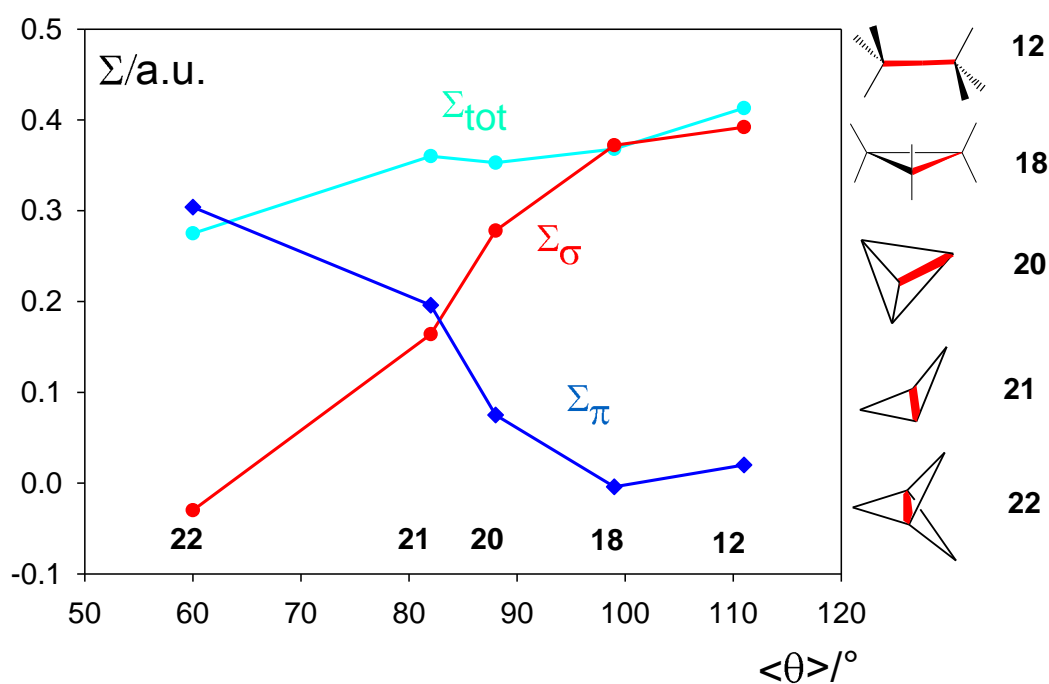


Figure 14. Various Σ values (a.u.) for ethane and a series of three-membered cyclic molecules (red bond).

Σ_{σ} decreases monotonously from 0.392 a.u. in ethane down to ca. zero for propellane, as previously noted.¹ But at the same time, this decrease is compensated in a large extent by an increase of Σ_{π} for **20**, **21** and **22**. As a matter of fact, the presence of two CH bridges in **20**, two and three CH_2 bridges in **21** and **22** respectively, allows the formation of “banana bonds” of π character.

From a panel of formally multiple bonds, we report in Table 7 the values of Σ_{tot} , Σ_{σ} , Σ_{π} (a.u.) and the mean angle $\langle\theta\rangle$ calculated for the σ component of the bond according to the method presented in section 2.1. For benzene **24**, $\langle\theta\rangle = 100^\circ$ is the mean of the two values of each Kékulé structure.

The Σ_{tot} ranges from 0.479 a.u. to 0.579 a.u. for double bonds, from 0.577 a.u. to 0.616 a.u. for triple bonds and is 0.480 a.u. for the “half double bond” of benzene. As expected, Σ_{tot} is slightly less in the conjugated **28** and **31** than in the corresponding non conjugated **27** and **32**.

Table 7. Values of Σ_{tot} , Σ_{σ} , Σ_{π} (a.u.) for CC bonds in multiple bonds and the corresponding values of $\langle\theta\rangle$ ($^\circ$) for their σ bond ($=\text{C}_3\text{H}_4$: cyclopropylidene, cf. Figure 16).

label	molecule	Σ_{tot}	Σ_{σ}	Σ_{π}	% π	$\langle\theta\rangle$
23	$\text{H}_2\text{C}=\text{C}=\text{CH}_2$	0.516	0.315	0.201	39.0	100
24	C_6H_6	0.480	0.342	0.139	29.9	100 ^a
25	$\text{H}_4\text{C}_3=\text{C}_3\text{H}_4$	0.537	0.320	0.217	34.0	97
26	$\text{CH}_2=\text{C}_3\text{H}_4$	0.479	0.283	0.196	40.9	90
27	$\text{H}_2\text{C}=\text{CH}_2$	0.521	0.267	0.254	48.8	81
28	$\text{CH}_2=\text{CH}-\text{CH}=\text{CH}_2$	0.488	0.256	0.232	52.6	80
29	cyclobutene	0.519	0.283	0.236	45.5	77
30	cyclopropene	0.579	0.277	0.304	52.5	71.5
31	$\text{HC}\equiv\text{C}-\text{C}\equiv\text{CH}$	0.577	0.159	0.418	72.4	60
32	$\text{HC}\equiv\text{CH}$	0.616	0.145	0.471	76.5	60
33	cyclopentyne	0.524	0.087	0.437	83	40

^a Mean value of the two Kékulé structures

From their $\langle\theta\rangle$ values, the σ part of the double and triple bonds can be considered as inverted bonds, except **23**, **24** and **25**. Indeed their Σ_{σ} values are smaller than that of cyclopropane **18** (0.372 a.u.). Their variations as a function of $\langle\theta\rangle$ are shown in Figure 15 with the same scale as in Figure 12 for ease of comparison. Like in formally single bonds, Σ_{σ} tends to decrease with $\langle\theta\rangle$, but with a weaker slope.

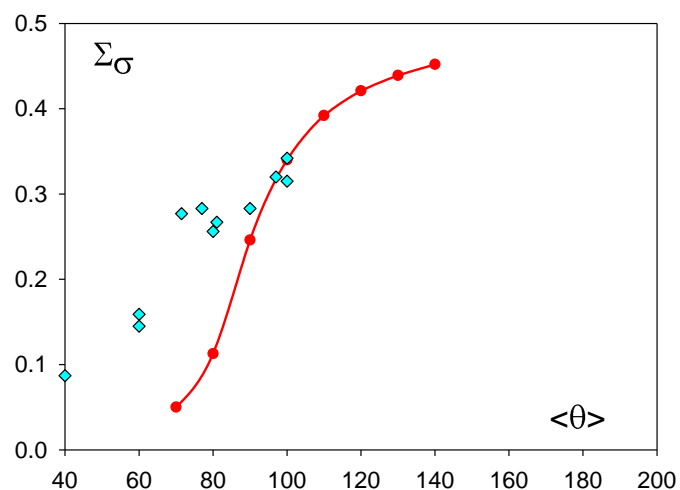


Figure 15. Values of $\Sigma\sigma$ (a.u.) for the σ bond in the formally multiple bond compounds 22-32 (cyan diamonds). The red curve corresponds to C_2H_6 model 1 for comparison.

The series **25**, **26** and **27** is illustrative of the influence of bond angles on σ bonds in formally double bonds (Figure 16).

	Σ_{tot}	$\Sigma\sigma$	$\Sigma\pi$	R(CC)	$\langle\theta\rangle$	
	25	0.537	0.354	0.183	1.316	97
	26	0.479	0.283	0.196	1.323	90
	27	0.521	0.267	0.254	1.332	81

Fig. 16. Some properties of the central bond in alkenes 24, 25 and 26 : Σ (a.u.), R(CC) (\AA) and $\langle\theta\rangle$ ($^\circ$).

The presence of two cyclopropenyl in **25** tends to increase $\langle\theta\rangle$ and $\Sigma\sigma$, which decreases in **26** and **27**. The same evolution is observed from cyclobutene **29** (R(CC) = 1.350 \AA) to cyclopropene **30** (R(CC) = 1.299 \AA).

The σ bonds of alkynes possess formally three C substituent at 0° and thus are strongly inverted. Because cyclopropyne and cyclobutyne are unstable, cyclopentyne **33** appears to

possess a σ bond with the smaller possible $\langle\theta\rangle$ value (40°) and thus the weaker Σ_σ (0.087 a.u.). As a result, in alkynes, the σ participation is no more than ca. 25% (whereas it is generally close to 50% in alkenes, which has been already remarked).¹³ In turn, the small $\langle\theta\rangle$ value for σ in triple bonds entails for $\langle\theta\rangle(\text{CH})$ its maximum theoretical value of 180° in **31** and **32**, in agreement with high CH bond dissociation in acetylene and hydrogen cyanide.

Conclusion

The dissociation energy BE of A-A bonds of $\text{AH}_n\text{-AH}_n$ with respect to geometry frozen AH_n is strongly dependant of the $\theta = \text{HAA}$ angles, exhibiting a sigmoidal variation: BE decreases rapidly when θ decreases to yield an “inverted bond” ($\theta < 90^\circ$) and tends to zero for $\theta = 60\text{-}70^\circ$. On the contrary if θ increases above its equilibrium value, BE increases. We propose the term of “superdirect” for this type of bond. The energy of a C-H bond in CH_4 as a function of the three other HCH angles behaves similarly. Within MO framework, this general behaviour is closely related to the s participation in the s+p hybrid AOs overlapping along the bond: it increases with θ from negative values in the inverted AH_n moiety ($\theta < 90^\circ$), to positive high values for $\theta > 90^\circ$.

The degree of invertedness/directness/superdirectness for any CC sigma bond can be characterised by the mean value $\langle\theta\rangle$ of its substituent angles, the π bonds being formally treated as σ ones. The sums of dynamic orbital forces (DOF), as indices of intrinsic bond energy and allowing their σ/π partition, are correlated to $\langle\theta\rangle$ in a panel of 33 molecules. The $\langle\theta\rangle$ parameter of a sigma CC bond thus appears as a simple and quite reliable index of its intrinsic strength. Concerning formally single bonds, it accounts, among others, for the strain energy of cyclanes. Also in the series cyclopropane, bicyclobutane, tetraedrane and propellane, it is shown that the strength of the bond common to several 3-membered cycles decreases with $\langle\theta\rangle$ from cyclopropane ($\langle\theta\rangle = 99^\circ$) to vanish in [1.1.1]propellane ($\langle\theta\rangle = 60^\circ$). At the opposite, the strongest σ CC bonds are found in butadiyne ($\langle\theta\rangle = 180^\circ$) and bonds having tetrahedryl and/or ethynyl substituent(s) ($\langle\theta\rangle > 120^\circ$). The method applies also to σ bonds in formally multiple bonds. These systems correspond to small $\langle\theta\rangle$ values so that such σ bonds can be considered as inverted in most of double bonds and in all the triple ones; thus they are significantly weaker than in standard formally single bonds.

References

-
- ¹ R. Laplaza, J. Contreras-Garcia, F. Fuster, F. Volatron, P. Chaquin, *Chem. Eur. J.* **2020**, *26*, 6839-6845.
- ² a) K. B. Wiberg, F.H. Walker, *J. Am. Chem. Soc.* **1982**, *104*, 5239-5240. b) D. Feller, E. R. Davidson, *J. Am. Chem. Soc.* **1987**, *109*, 4133-4139. c) J. E. Jackson, L. C. Allen, *J. Am. Chem. Soc.* **1984**, *106*, 591-599.
- ³ W. Wu, J. Gu, J. Song, S. Shaik, Hiberty, P. C., *Angew. Chem.* **2009**, *121*, 1435–1438.
- ⁴ B. Braïda, S. Shaik, W. Wu, P. C. Hiberty, *Chem. Eur. J.* **2020**, *26*, 5935-6939.
- ⁵ Gaussian 09, Revision A.01, M. J. Frisch, G. W. Trucks, H. B. Schlegel, G. E. Scuseria, M. A. Robb, J. R. Cheeseman, G. Scalmani, V. Barone, B. Mennucci, G. A. Petersson, H. Nakatsuji, M. Caricato, X. Li, H. P. Hratchian, A. F. Izmaylov, J. Bloino, G. Zheng, J. L. Sonnenberg, M. Hada, M. Ehara, K. Toyota, R. Fukuda, J. Hasegawa, M. Ishida, T. Nakajima, Y. Honda, O. Kitao, H. Nakai, T. Vreven, J. A. Montgomery, Jr., J. E. Peralta, F. Ogliaro, M. Bearpark, J. J. Heyd, E. Brothers, K. N. Kudin, V. N. Staroverov, R. Kobayashi, J. Normand, K. Raghavachari, A. Rendell, J. C. Burant, S. S. Iyengar, J. Tomasi, M. Cossi, N. Rega, J. M. Millam, M. Klene, J. E. Knox, J. B. Cross, V. Bakken, C. Adamo, J. Jaramillo, R. Gomperts, R. E. Stratmann, O. Yazyev, A. J. Austin, R. Cammi, C. Pomelli, J. W. Ochterski, R. L. Martin, K. Morokuma, V. G. Zakrzewski, G. A. Voth, P. Salvador, J. J. Dannenberg, S. Dapprich, A. D. Daniels, Ö. Farkas, J. B. Foresman, J. V. Ortiz, J. Cioslowski, D. J. Fox, Gaussian, Inc., Wallingford CT, **2009**
- ⁶ A. Krapp, F. M. Bickelhaupt, G. Frenking, *Chem. Eur. J.* **2006**, *12*, 9196-9216.
- ⁷ Y. Yamaguchi, B. C. Hoffman, J. C. Stephens, H. F. Schaefer, *J. Phys. Chem. A* **1999**, *103*, 38, 7701–7708
- ⁸ a) M. J. S. Dewar, H. N. Schmeising, *Tetrahedron* **1959**, *5*, 166.; b) R. A. Alden, J. Kraut, T. G. Traylor, *J. Am. Chem. Soc.* **1968**, *90*, 74; c) S. Osawa, M. Sakai, E. Osawa, *J. Phys. Chem. A* **1997**, *101*, 1378. d) M. G. Brown *Trans. Faraday Soc.*, **1959**, *55*, 694-700.
- ⁹ Tanaka, M.; Sekiguchi, A. *Angew. Chem., Int. Ed.* **2005**, *44*, 5821
- ¹⁰ F.W. Averill, G. S Painter, *Phys. Rev. B* **1986**, *34(4)* 2088-2095
- ¹¹ a) T. Tal, J. Katriel, *Theoret. Chim. Acta* **1977**, *46*, 173-181; b) F.M.Bickelhaupt, J. K. Nagle, W.L. Klemm, *J. Phys. Chem. A* **2008**, *112*, 2437-2446; c) P. J. Robinson, A.N. Alexandrova, *J. Phys. Chem. A* **2015**, *119*, 12862–12867. d) P. Chaquin, Y. Canac, C. Lepetit, D. Zargarian, R. Chauvin, *Int. J. Quant. Chem.* **2016**, *116*, 1285-1295; e) P. Chaquin, F. Fuster, F. Volatron, *Int. J. Quant. Chem* **2018**, *118*, 25658-25659
- ¹² a) Y. Yamaguchi, R.B. Remington, J.F. Gaw, H. F. Schaefer III, G. Frenking, *Chem. Phys.* **1994**, *180*, 55-70; b) Y. Yamaguchi, R.B. Remington, J.F. Gaw, H. F. Schaefer III, G. Frenking, *J. Chem. Phys.* **1993**, *98* (11), 8749-8760; c) Yamaguchi, B. J. DeLeeuw, C. A. Richards, Jr., H. F. Schaefer III, G. Frenking. *J. Am. Chem. Soc.* **1994**, *116*, 11922-11930.
- ¹³ F. Fuster, P. Chaquin, *Int. J. Quant. Chem* **2019**, *119* (20), e25996
- ¹⁴ Y. Mo, *Org. Lett.* **2006**, *8*(3), 535-538.

¹⁵ a) I. Fernandez, G. Frenking, *Chem. Eur. J.* **2006**, *12*, 3617 – 3629; b) G. Gayatri, Y. Soujanya, I. Fernández, G. Frenking, G. Narahari Sastry, *J. Phys. Chem. A* **2008**, *112*, 12919–12924.

¹⁶ J. Blanksby, G. B. Ellison, *Acc. Chem. Res.* **2003**, *36*, 4, 255–263

¹⁷ a) K. W. Wiberg, *Angew. Chem. Int. Ed. Eng.* **1986**, *25*, 312-322; b) K. W. Wiberg, R.A. Fenoglio, *J. Am. Chem. Soc.* **1968**, *90*, 3395-3397.

¹⁸ a) K. Exner, P.v. R. Schleyer, *J. Phys. Chem. A* **2001**, *105*, 3407- 3416; b) R. D. Bach, O. Dimitrenko, *J. Org. Chem.* **2002**, *67*, 3884-3896; c) R. D. Bach, O. Dimitrenko,, *J. Org. Chem.* **2002**, *67*, 2588-2599; c) S. Grimme, *J. Am. Chem. Soc.* **1996**, *118*, 1529-1534.

¹⁹ R. D. Bach, O. Dimitrenko, *J. Am. Chem. Soc.* **2004** *126*, 4444-4452.